



THE UNIVERSITY *of* EDINBURGH
School of Physics
and Astronomy

Superconductivity in 3d metal Hydrides

Guilherme Garcia s2240769
September 2024

Abstract

Several studies have shown the superconducting properties of 3d metal Hydrides (Mn, Fe, Co, Ni). When looking at the different crystal structures of these hydrides some repeat across different metals. This project aimed to provide a systematic analysis of the formation of 3d metal hydrides using first principles electronic structure calculations. Convex Hulls for each of the metal hydrides were calculated and several structures were tested across the different metals to look for possible trends in their formation. A new stable form, NiH_5 , seems to have been found, however, further studies need to be made to confirm this result. An unsuccessful attempt was made to calculate the superconducting T_c of the stable structures found. Further studies should perform a structure optimization step before attempting to calculate the superconducting T_c for the stable compounds.

Lay Summary

Superconducting materials have a wide range of applications, from superconducting magnets in particle accelerators and MRI machines to transportation or quantum computing. However, these materials only gain the properties that make them so useful at very low temperatures, which are very hard to reach. As such, the search for room-temperature superconductors has become one of the most interesting scientific endeavours to pursue. In this project, I took several known forms of superconducting materials within the same region in the periodic table and tried to provide a systematic study to test if by swapping the type of metal present on the structure, a new superconducting system could be found.

Personal Statement

This project provided me with the opportunity to apply the theoretical knowledge I had learned throughout my degree as well as further expand it and gain practical research experience. Throughout this project, I was introduced to the field of condensed matter and got to learn more about Density Functional Theory and its practical implementation which has led me to improve my independent research skills as well as my time management skills. Furthermore, it allowed me to develop my coding skills, allowing me to learn more about bash scripts and parallel computing as well as helping me quickly learn how to work with new and unfamiliar software. Above all, this project allowed me to experience an academic research environment and learn more about a new area of physics I didn't know before.

Contents

1	Introduction	1
2	Theory	2
2.1	Schrodinger’s Equation for an N-Body system	2
2.2	Density Functional Theory	3
2.3	Superconductivity	5
3	Methods	5
3.1	Convex Hull Analysis	5
3.2	T _c Calculation	6
4	Results & Discussion	7
4.1	Convex Hull Analysis	7
4.2	T _c Calculations	9
5	Conclusion	10
6	Acknowledgements	10
	References	10
A	Structures	12
B	Code examples	14
B.1	VASP	14
B.1.1	Job Script	14
B.1.2	INCAR	16
B.1.3	KPOINTS	17
B.2	Quantum Espresso	17
B.2.1	SCF Calculation	17
B.2.2	Phonon Calculation	18
B.2.3	Post Processing Calculations	19
C	Densities of States	20

1 Introduction

Recent studies have demonstrated the superconducting potential of hydrides of 3d transition metals (Mn, Fe, Co, Ni) [1] [2] [3] [4]. A quick look at the structures for the different compounds shows repeated structures across compounds of different elements. This project aims to provide a systematic overview of the relations between these different compounds by cross-analysing the different structures found to be stable for each compound across all the other compounds. After the determination of the Convex Hull for each compound across a comprehensive range of pressures, we aimed to determine the superconducting T_c of the stable structures.

A stable form of NiH_5 seems to have been found, however further analysis is needed to rule out the possibility of this being a computational error. Our attempt at calculating the T_c for the different stable structures was unsuccessful, repeatedly finding negative values for the electron-phonon coupling constant.

To properly calculate the superconducting T_c , a new calculation must be made, this time including a structure optimization cycle in order to correct potential numerical errors between the software used to find the stable structures (VASP) and the one used to perform the superconductivity calculations (Quantum Espresso). Further studies could focus on cross testing some of the structures that could not be tested during this project (see missing structures in Table 1) or studying some of the interesting phenomena found during this analysis.

2 Theory

Although this project is mainly computational, it is important to understand the theory behind the methods used in it. As such this section aims to summarise the key points of the theory used in this project in a way that someone not familiar with this field can understand what has been done.

2.1 Schrodinger's Equation for an N-Body system

To find the optimal structure for a given compound, one needs to solve an N-Body Schrodinger's equation corresponding to the system. However, the difficulty of this equation increases exponentially as we add more atoms in our system. As such there are several approximations that must be used to simplify the system and make it solvable.

When considering an N-Body system, the basic equation we need to solve can be written as:

$$E_{tot}\psi = \left[-\sum_i \frac{\hbar^2}{2m_e} \nabla_i^2 - \sum_I \frac{\hbar^2}{2M_I} \nabla_I^2 + \frac{1}{2} \sum_{i \neq j} \frac{e^2}{4\pi\epsilon_0} \frac{1}{|\mathbf{r}_i - \mathbf{r}_j|} + \frac{1}{2} \sum_{I \neq J} \frac{e^2}{4\pi\epsilon_0} \frac{Z_I Z_J}{|\mathbf{R}_I - \mathbf{R}_J|} - \sum_{i,I} \frac{e^2}{4\pi\epsilon_0} \frac{Z_I}{|\mathbf{r}_i - \mathbf{R}_I|} \right] \psi \quad (1)$$

The first two terms represent the kinetic energy of the electrons (m_e is electrons mass) and the nuclei (M_I is nucleus mass) of the system. The last 3 terms represent the electron-electron, nucleus-nucleus and electron-nucleus potential energies [5].

This equation is too complicated to be solved analytically or numerically and thus some approximations must be done to make this problem solvable. By applying the Bohr Oppenheimer (in a solid we assume that the nucleus does not change position), the independent electrons (each electron can be treated as being independent of each other) and the mean field (reintroducing part of the effect of the electronic repulsion while keeping the simplification from the independent electrons approximation, by introducing an electrostatic potential that represents the mean kinetic energy the electrons would feel from the electronic repulsion) approximations, we can obtain the Hartree equations:

$$\left[-\frac{\nabla^2}{2} + V_n(\mathbf{r}) + V_H(\mathbf{r}) \right] \phi_i = \epsilon_i \phi_i \quad (2)$$

$$n(\mathbf{r}) = \sum_i |\phi_i(\mathbf{r})|^2 \quad (3)$$

$$\nabla^2 V_H(\mathbf{r}) = 4\pi n(\mathbf{r}) \quad (4)$$

Where V_H is known as the Hartree potential and represents the mean field caused by the electronic density ($n(\mathbf{r})$) and V_n is the potential caused by the nucleus in the atom (this can be considered a constant since we assume the positions of the nucleus don't change). These are a set of simultaneous equations that can be solved iteratively by a computational loop, however, these seem to ignore the quantum nature of the electrons. As such, there are two more approximations we must include.

Firstly the spin of the electrons must be accounted for, as well as the fact that these must obey Pauli's exclusion principle (and be in the form of a Slater determinant). This can be done by adding a new non-local potential, the Fock exchange potential ($V_x(\mathbf{r}, \mathbf{r}')$), in the single particle equation (equation 2) to account for these effects. However, this can be replaced by a simplified exchange potential ($V_x(\mathbf{r})$) that keeps a good approximation of this effect and removes the need for more complicated non-local calculations.

Lastly, we need to account for the effects of the Coloumb repulsion when finding electrons in a given location (ie. if there is an electron in a given region, the likelihood of finding an electron close to it is smaller than the probability of finding an electron in an empty region). This can be accounted for by adding another potential, the correlation potential ($V_c(\mathbf{r})$).

Adding these two extra factors gives us the Kohn-Sham equations:

$$\left[-\frac{\nabla^2}{2} + V_n(\mathbf{r}) + V_H(\mathbf{r}) + V_x(\mathbf{r}) + V_c(\mathbf{r}) \right] \phi_i = \epsilon_i \phi_i \quad (5)$$

$$n(\mathbf{r}) = \sum_i |\phi_i(\mathbf{r})|^2 \quad (6)$$

$$\nabla^2 V_H(\mathbf{r}) = 4\pi n(\mathbf{r}) \quad (7)$$

These are still a set of 3 simultaneous equations and correspond to an accurate description of the quantum nature of our system, however we do not have a form for the exchange and correlation potentials.

2.2 Density Functional Theory

Density Functional Theory (DFT) attempts to use a computationally effective method to solve the Kohn-Sham equations.

Firstly we can start by stating that the total energy of a quantum mechanical system is in fact a functional of the wave function that describes that system.

$$E = \langle \Psi | \hat{H} | \Psi \rangle = F[\Psi] \quad (8)$$

Now if we consider the energy of the ground state of our system (which is exactly what we are considering when studying a stable solid), we can make use of the Hohenberg-Kohn theorem. This states that for the ground state of a system, its electron density completely determines the properties of the system [5]. This means that we can express the total energy of the system as a functional of the electronic density: $E = F[n(\mathbf{r})]$.

Using this information we can write the Kohn-Sham equation for a single particle:

$$\left[-\frac{\nabla^2}{2} + V_n(\mathbf{r}) + V_H(\mathbf{r}) + V_{xc}(\mathbf{r}) \right] \phi_i = \epsilon_i \phi_i \quad (9)$$

Where V_{xc} combines both the exchange and correlation potentials and can be described as :

$$V_{xc}(\mathbf{r}) = \left. \frac{\delta E_{xc}[n]}{\delta n} \right|_{n(\mathbf{r})} \quad (10)$$

Where $E_{xc}[n]$ is the exchange-correlation energy. If we have a form for this energy, we can then get all the energy for the whole system, since all the other aspects of the energy are well-known. There are different approximations for the form of $E_{xc}[n]$, however, we will not discuss this in this report, for more information see Ref.[5].

To find the total energy of a system, DFT calculations perform what is called a Self Consistent Field, that iteratively solves the Kohn-Sham equations (equations 9, 6, 7 and 10) using an initial ansatz for the electronic density field and repeating the calculation until the difference between the initial and final results is within an acceptable threshold (see fig.B.2.1).

Using the SCF method to calculate the minimum energy for a given atomic structure allows us to perform several structural calculations. This includes structure optimizations, where a program is capable of finding the atomic positions that minimize the energy for a given structure.

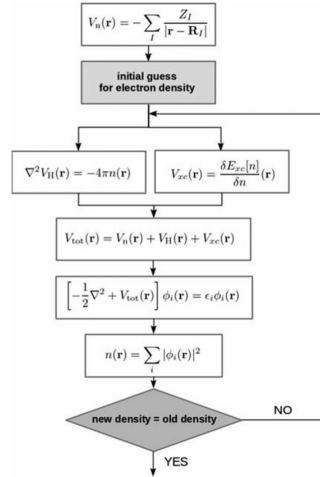


Figure 1: Scheme of a Self Consistent Field calculation used in DFT [5]

2.3 Superconductivity

Superconductivity happens when, below a given temperature T_c , the material's resistance drops to zero [6]. This project will be studying Type I superconductivity, where the material exhibits the Meissner effect (perfect diamagnetism, $B=0$) and whose formation mechanism is well known. This mechanism is called phonon mediated super-conductivity, where below T_c , the electrons in the material will form cooper pairs that no longer need to obey the Pauli exclusion principle. Through this the electrons can occupy the ground state, no longer interacting with the rest of the system and thus bringing the resistance to zero.

The superconducting T_c for this type of superconductor can be estimated using BCS theory and the MacWilliam-Allen-Dyes equation (equation 11) [7] :

$$T_c = \frac{\omega_{log}}{1.2} \exp \left(-\frac{1.04(1 + \lambda)}{\lambda - \mu^*(1 + 0.62\lambda)} \right) \quad (11)$$

$$\lambda = 2 \int \frac{\alpha^2 F(\omega)}{\omega} d\omega, \quad \omega_{log} = \exp \left[\frac{2}{\lambda} \int_0^\infty \frac{d\omega}{\omega} \alpha^2 F(\omega) \ln(\omega) \right] \quad (12)$$

$$\alpha^2 F(\omega) = \frac{1}{2\pi N(\epsilon_f)} \sum_{i\mathbf{q}} \frac{\gamma_{\mathbf{q}i}}{\omega_{\mathbf{q}i}} - \delta(\omega - \omega_{\mathbf{q}i}) \omega(\mathbf{q}) \quad (13)$$

Where ω_{log} is the logarithmic average of the phonon frequencies and λ is the electron-phonon coupling constant (see equation 12). These values are given by the Eliashberg function $\alpha^2 F(\omega)$ (equation 13), which gives the electron-ion induced phonon broadening in terms of the phonon linewidth $\gamma_{\mathbf{q}i}$, for of wave vector \mathbf{q} in mode i . μ^* is the Coulumb Pseudopotential, which is found empirically (for example for Fe-H systems this should traditionally be between 0.1 and 0.15 [2]).

3 Methods

3.1 Convex Hull Analysis

This project used computational methods to first find the convex hull of stable structures for hydrides of each 3d metal and then tested its stable structures for superconductivity.

To perform the convex hull analysis, we used VASP ("The Vienna Ab initio Simulation Package") [8] [9] to perform a structure optimization across a range of different pressures, usually between 0.01 KBar and 3000 KBar. We started by using a structure from a literature source as the starting structure for the first pressure point and then performed a structure optimization across the whole pressure range, using the optimized structure from the previous pressure point as the beginning structure for the next pressure point (see sections B.1.1 and B.1.2). The same K-Grid was used across all the calculations in order to keep consistency (see section B.1.3). A full list of the structures studied and where their initial structure was found can be found in section A.

Once VASP has found the stable structure at each pressure point, it returned its corresponding minimum energy as well. This energy was treated as an enthalpy, since although VASP returns a Free Energy, it only considers in this calculation the entropy

from the smearing of the electron occupancies, ignoring all other, more relevant contributions to the entropy of this system, meaning we should just assume this entropy is too small to be considered and treat the value from VASP as an enthalpy instead.

To compare different structures, these are first normalized per unit structure (per H atom in the case of hydrogen, or per M_xH_y unit structure for the other hydrides). Following this, we calculate the change in enthalpy to construct the complex hull.

$$\Delta H = \frac{1}{n}(H_f(MH_n) - H_f(MH) - (n-1)H_f(H)) \quad (14)$$

Equation 14 shows the calculation for the enthalpy change for a monohydride. It calculates the enthalpy change of the compound when compared with the expected values for its individual components, if this value is negative then the compound will form. The convex hull is formed by the line that joins together the compounds with the smallest ΔH . If a compound can be found in the convex hull, it will be stable. If a compound is up to 0.03 eV/atom above the convex hull, it is considered to be meta-stable (see Figure 2).

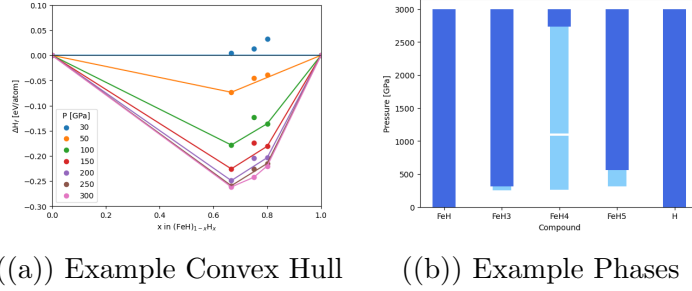


Figure 2: Example Convex Hull and Compounds Phases from the initial results of the Fe study

3.2 T_c Calculation

To calculate the superconducting T_c , we used Quantum Espresso [10] [11]. Using the data from the Convex Hulls, for each element, we selected the pressure point with most stable structures to perform the T_c calculations (700 KBar for the case of Fe).

For each of the stable structures we started by running a new SCF cycle, this time using Quantum Espresso to calculate the material's Density of States and check its potential for superconductivity. After checking that the material presents a metallic behaviour, we performed a second SCF calculation (see section B.2.1), to obtain the values for the phonon calculation (see section B.2.2), this used Density Functional Perturbation Theory to determine the electron-phonon coupling parameters [7]. At last, we performed several post-processing calculations (see section B.2.3) to get the parameters to calculate T_c using the MacWilliam-Allen-Dyes equation (equation 11).

4 Results & Discussion

4.1 Convex Hull Analysis

The summary of all the structures studied during the project can be found in table 1. When there was a literature source that described a structure with the space group, we went with the structure described in that paper (thus the different sources for the same element), whenever there wasn't a literature reference for that element we replaced the metallic atoms from the source lattice with the metal of the hydride being studied (further information on which literature source was used for each structure can be found on Appendix A).

On the convex hull plots, the triangles represent compounds without a literature source behind them (adapted from the structure of other metals). On the Compounds Stability plot, dark blue represents stability and light represents meta-stability.

Structure	Space Group	Origin Hydride - Source	Mn	Fe	Co	Ni
MH	P63/mcm	Mn - [1]	Tested	-	-	-
	Fm $\bar{3}$ m	Fe - [12] Co - [13] Ni - [4]	-	Tested	Tested	Tested
MH ₂	I4/mmm	Mn - [1] Co - [13]	Tested	-	Tested	Tested
	Immm	Fe - [2]	-	Tested	-	-
	Fm $\bar{3}$ m	Co - [13]	-	-	Tested	Tested
MH ₃	I4/m	Mn - [1]	Tested	-	-	-
	Pm $\bar{3}$ m	Fe - [12] Mn - [13]	Tested	Tested	Tested	Tested
	Pm $\bar{3}$ n	Fe - [12]	-	-	Tested	Tested
MH ₄	Pm/3m	Mn - [1]	Tested	-	-	-
	Cmmm	Fe - [14]	-	Tested	Tested	Tested
	Immma	Fe - [15]	-	Tested	Tested	Tested
	P21m	Fe - [12]	-	Tested	Tested	Tested
	P213	Fe - [15]	-	Tested	Tested	Tested
MH ₅	I4/mmm	Fe - [2] [14]	Tested	Tested	Tested	Tested
MH ₆	C2/m	Fe - [2]	Tested	Tested	Tested	Tested
	Cmmm	Fe - [2]	Tested	Tested	Tested	Tested
MH ₇	P63mcm	Mn - [1]	Tested	-	-	Tested
	P63mmm	Mn - [1]	Tested	-	-	Tested
MH ₈	P $\bar{1}$	Mn - [1]	Tested	-	-	Tested
M ₂ H ₃	I2/m	Ni - [4]	-	-	Tested	Tested
M ₃ H ₅	Pmmm	Fe - [2]	-	Tested	-	Tested
M ₃ H ₈	Pm $\bar{3}$ m	Fe - [2]	-	Tested	-	Tested
M ₃ H ₁₃	I4/mmm	Fe - [2]	-	Tested	-	Tested

Table 1: Structures tested

The convex hull and the stable structures for Manganese can be found in figure 3. Most of the results for the known compounds seem to be in accordance with the literature results, with the exception of MnH₈, which should be stable or meta-stable.

Throughout this study, the structure MH₅ from Ref.[14] has seemed to cause some errors and hinted at a phase transition into a new stable structure, however using the

same structure and space group, but with the data from Ref.[2] showed no problem whatsoever. We proceeded to make a more detailed study of this phenomenon for the Manganese compound. We did this by taking a structure file from after the apparent phase transition had happened and used it as an input for a new structure optimization to try to get a complete set of data for this new structure. However, when analysing the new results, it seemed to have formed an MnH6 structure, which should not be possible. A further analysis must be conducted into this to properly understand this phenomenon.

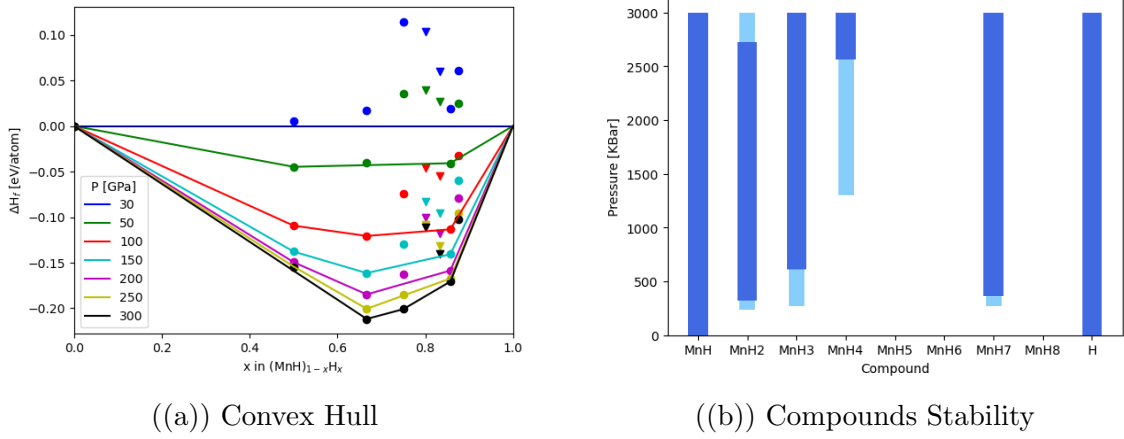


Figure 3: Manganese Convex Hull and Compounds Stability

No new structures were tested for Iron compounds, as can be seen in Figure 4. However, the results in the convex hull seem to be in agreement with the literature values. The same phenomenon with the FeH_5 structure was observed too.

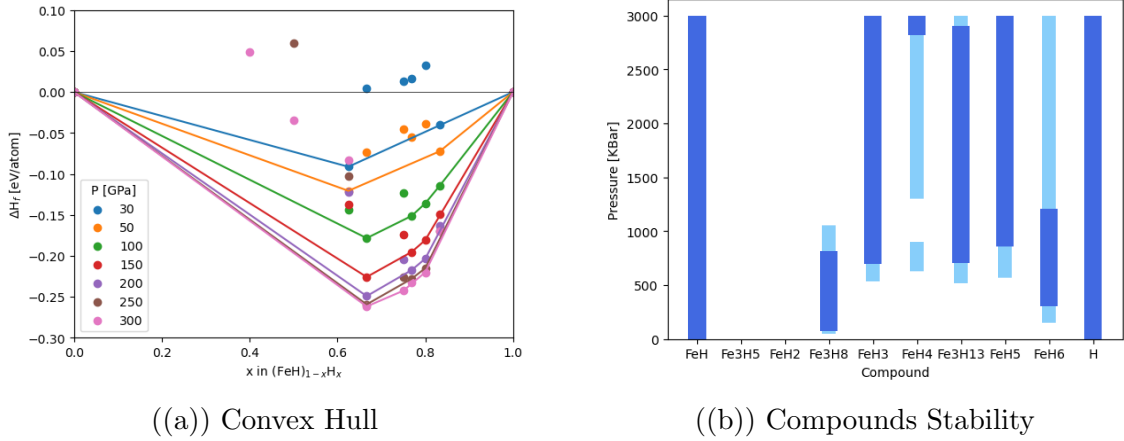


Figure 4: Iron Convex Hull and Compounds Stability

Cobalt's structures based on literature values seem to agree with it, as shown by Figure 7. No new stable structures were found using this method, although a short metastability seems to have formed at the CoH_8 structure.

Ref.[3] also seems to indicate the existence of a 3rd form CoH_2 , CoH_2 $P4nmm$ at high pressures that seems to be relevant for this study, however, we were not able to find

the formula for this. A further development in this study could involve including this and other potential structures that could be found in a future literature review, in this analysis.

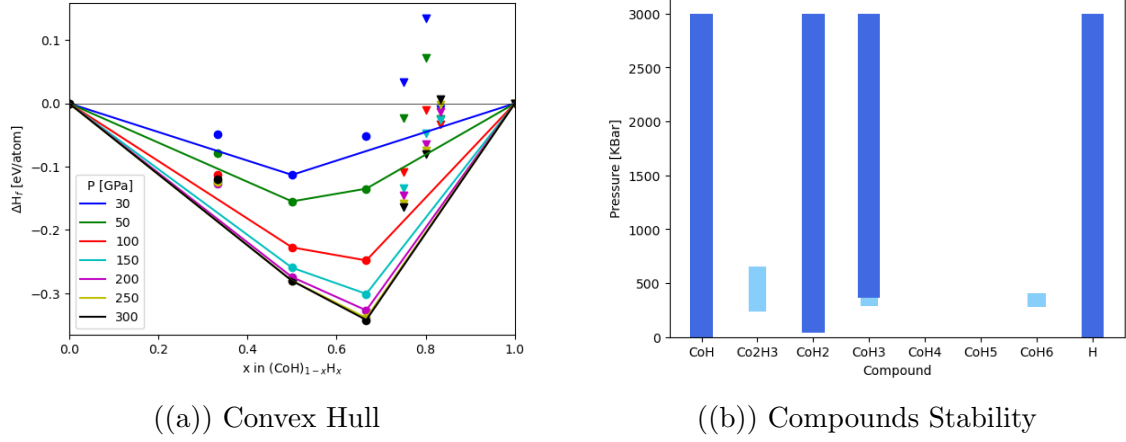


Figure 5: Cobalt Convex Hull and Compounds Stability

The Nickel Convex Hull (shown in Figure 6) was only calculated for pressures up to 200 GPa to reduce the computational power needed to calculate the structures being studied. The results seem to indicate new stable forms at NiH_2 and NiH_5 . However, the NiH_2 has been predicted by other literature sources that have not been used to find base structures for this study [16] [17]. Although this result is not novel, this confirms the suitability of this method to find potential new stable structures.

As for the new stable structure that seems to have been found at NiH_5 , this might be just because of the known MH_5 effect. Another calculation, this time based on the structure from Ref.[2] needs to be performed to confirm this result.

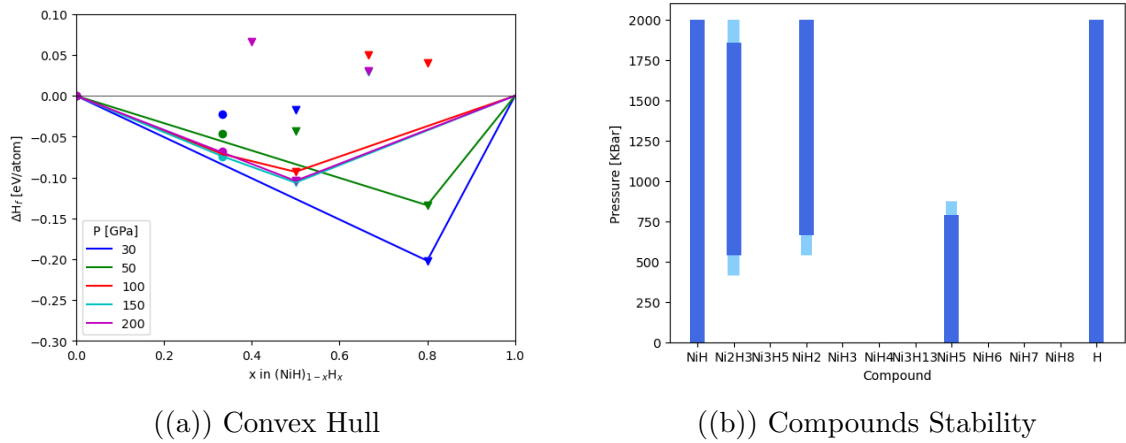


Figure 6: Nickel Convex Hull and Compounds Stability

4.2 Tc Calculations

An attempt was made to calculate the T_c values for the Iron stable structures at 700 KBar (pressure at which most stable structures existed). However, after performing the

phonon calculations for different Iron structures, they all showed negative electron-phonon coupling constant (λ) values when calculating the different phonon modes. This seems to indicate that there is either some problem with the way the calculations were run or that the structure used is not stable. A possible solution for this problem could be to run a new structure optimization cycle should be run before the SCF cycle in Quantum Espresso to ensure the structure used is stable.

The densities of states of the structures studied for T_c were calculated (see Appendix C for the DOS Plots) to confirm the metallicity of the structures before proceeding into further calculations. However, considering the results obtained for λ , these too must be recalculated after a structure optimisation to ensure the final structures remain metallic.

5 Conclusion

This project has tried to provide a systematic study of the 3d transition metal hydrides and the potential connections between the different stable structures across different metals. Further studies must be conducted to finalise this, since not all combinations of hydrides have been tested (see Table 1). Furthermore, further studies must be conducted to understand the behaviour of the MH_5 structure derived from [14] and a broader literature review could be conducted to make sure all possible structures have been included in this analysis.

At last, a new T_c calculation must be attempted to test if the new stable structures present superconductivity and at which temperatures. For this, the problems with the phonon calculations need to be solved. This must include a structure optimization step in the Quantum Espresso code to make sure the structures tested are in their stable form and avoid any potential discrepancies that may arise from differences between the VASP and Quantum Espresso code.

6 Acknowledgements

I would like to thank my supervisor Andreas Hermann for his help and guidance throughout this project. I would also like to thank Max Donaldson and Andrew Lyall for their advice and knowledge shared during this project. I am grateful to the UK Materials and Molecular Modelling Hub for computational resources, which is partially funded by EPSRC (EP/T022213/1, EP/W032260/1 and EP/P020194/1). I am also very grateful to the School of Physics and Astronomy for providing me with the Academic Development Scholarship that has allowed me to conduct this project.

References

1. Charraud, J.-B., Geneste, G. & Torrent, M. Manganese hydrides and superhydrides at high pressure. *Physical Review B* **100**, 224102. ISSN: 2469-9950, 2469-9969. <https://link.aps.org/doi/10.1103/PhysRevB.100.224102> (2024) (Dec. 3, 2019).

2. Kvashnin, A. G., Kruglov, I. A., Semenov, D. V. & Oganov, A. R. Iron Superhydrides FeH₅ and FeH₆ : Stability, Electronic Properties, and Superconductivity. *The Journal of Physical Chemistry C* **122**, 4731–4736. ISSN: 1932-7447, 1932-7455. <https://pubs.acs.org/doi/10.1021/acs.jpcc.8b01270> (2024) (Mar. 1, 2018).
3. Peña-Alvarez, M. *et al.* Synthesis of Superconducting Cobalt Trihydride. *The Journal of Physical Chemistry Letters* **11**, 6420–6425. ISSN: 1948-7185, 1948-7185. <https://pubs.acs.org/doi/10.1021/acs.jpclett.0c01807> (2024) (Aug. 6, 2020).
4. Binns, J. *et al.* Synthesis of Ni₂H₃ at high temperatures and pressures. *Physical Review B* **98**, 140101. ISSN: 2469-9950, 2469-9969. <https://link.aps.org/doi/10.1103/PhysRevB.98.140101> (2024) (Oct. 11, 2018).
5. Martin, R. M. *Electronic structure: basic theory and practical methods* 1. paperback ed. with corr., 5. pr. 624 pp. ISBN: 978-0-521-78285-2 978-0-521-53440-6 (Cambridge Univ. Press, Cambridge, 2011).
6. Rey, C. & Malozemoff, A. in *Superconductors in the Power Grid* 29–73 (Elsevier, 2015). ISBN: 978-1-78242-029-3. <https://linkinghub.elsevier.com/retrieve/pii/B9781782420293000029> (2024).
7. Hermann, A. Electronic Structure Theory - Course Notes. *2019/2020*.
8. Kresse, G. & Hafner, J. Ab initio molecular dynamics for liquid metals. *Phys. Rev. B* **47**, 558–561. <https://link.aps.org/doi/10.1103/PhysRevB.47.558> (1 Jan. 1993).
9. Kresse, G. & Furthmüller, J. Efficiency of ab-initio total energy calculations for metals and semiconductors using a plane-wave basis set. *Computational Materials Science* **6**, 15–50. ISSN: 0927-0256. <https://www.sciencedirect.com/science/article/pii/0927025696000080> (1996).
10. Giannozzi, P. *et al.* QUANTUM ESPRESSO: a modular and open-source software project for quantum simulations of materials. *Journal of Physics Condensed Matter* **21**, 395502. arXiv: 0906.2569 [cond-mat.mtrl-sci] (Sept. 2009).
11. Giannozzi, P. *et al.* Advanced capabilities for materials modelling with Quantum ESPRESSO. *Journal of Physics Condensed Matter* **29**, 465901. arXiv: 1709.10010 [cond-mat.mtrl-sci] (Nov. 2017).
12. Allers, K. N. & Liu, M. C. A NEAR-INFRARED SPECTROSCOPIC STUDY OF YOUNG FIELD ULTRACOOL DWARFS. *The Astrophysical Journal* **772**, 79. ISSN: 0004-637X, 1538-4357. <https://iopscience.iop.org/article/10.1088/0004-637X/772/2/79> (2024) (July 9, 2013).
13. Wang, L. *et al.* High-Pressure Formation of Cobalt Polyhydrides: A First-Principle Study. *Inorganic Chemistry* **57**, 181–186. ISSN: 0020-1669, 1520-510X. <https://pubs.acs.org/doi/10.1021/acs.inorgchem.7b02371> (2024) (Jan. 2, 2018).
14. Pépin, C. M., Geneste, G., Dewaele, A., Mezouar, M. & Loubeyre, P. Synthesis of FeH₅ : A layered structure with atomic hydrogen slabs. *Science* **357**, 382–385. ISSN: 0036-8075, 1095-9203. <https://www.science.org/doi/10.1126/science.aan0961> (2024) (July 28, 2017).

15. Li, F. *et al.* Structural evolution of FeH₄ under high pressure. *RSC Advances* **7**, 12570–12575. ISSN: 2046-2069. <https://xlink.rsc.org/?DOI=C6RA25591D> (2024) (2017).
16. Kanagaprabha, S., Meenaatci, A., Rajeswarapalanichamy, R. & Iyakutti, K. First Principles Study of the Electronic Structure, Structural Properties and Superconductivity of Nickel Hydride. *Walailak Journal of Science and Technology (WJST)* **9**, 115–126. <https://wjst.wu.ac.th/index.php/wjst/article/view/231> (Apr. 4, 2012).
17. Ying, J., Liu, H., Greenberg, E., Prakapenka, V. B. & Struzhkin, V. V. Synthesis of new nickel hydrides at high pressure. *Physical Review Materials* **2**, 085409. ISSN: 2475-9953. <https://link.aps.org/doi/10.1103/PhysRevMaterials.2.085409> (2024) (Aug. 31, 2018).
18. Code repository for this project. <https://github.com/Garcia242/Superconductivity-in-3d-Metal-Hydrides>.

A Structures

This section provides an exhaustive list of all the structures studied in this project as well as from where the initial structure was based of. The input files for these structures can be found in Ref. [18].

Compound	Space Group	source
MnH	P63/mmc	[1]
MnH ₂	I4/mmm	[1]
MnH ₃	I4/m	[1]
	Pm $\bar{3}$ m	Adapted from Fe structure from Ref.[12]
MnH ₄	Pm/3m	[1]
MnH₅	I4/mmm	Adapted Fe structure from Ref.[14]
MnH ₆	C2/m	Adapted from Fe structure from Ref.[2]
	Cmmm	Adapted from Fe structure from Ref.[2]
MnH ₇	P63mcm	[1]
	P63mmn	[1]
MnH ₈	P $\bar{1}$	[1]

Table 2: Mn Structures Studied

Compound	Space Group	source
FeH	Fm $\bar{3}$ m	[12]
FeH ₂	Immm	[2]
FeH ₃	Pm $\bar{3}$ m	[12]
	Pm $\bar{3}$ n	[12]
Fe ₃ H ₅	Pmmm	[2]
Fe ₃ H ₈	Pm $\bar{3}$ m	[2]
FeH ₄	Cmmm	[14]
	Immma	[15]
	P21m	[12]
	P213	[15]
Fe ₃ H ₁₃	I4/mmm	[2]
FeH ₅	I4/mmm	[2]
FeH ₆	C2/m	[2]
	Cmmm	[2]

Table 3: Fe Structures Studied

Compound	Space Group	source
CoH	Fm $\bar{3}$ m	[13]
CoH ₂	Fm $\bar{3}$ m	[13]
	I4/mmm	[13]
CoH ₃	Pm $\bar{3}$ m	[13]
CoH ₄	Cmmm	Adapted from Fe structure in Ref.[14]
	Immma	Adapted from Fe structure in Ref.[15]
	P21m	Adapted from Fe structure in Ref.[12]
	P213	Adapted from Fe structure in Ref.[15]
CoH ₅		Adapted from Fe structure from Ref.[2]
CoH ₆	Cmmm	Adapted from Fe structure from Ref.[2]
	C2/m	Adapted from Fe structure from Ref.[2]
Co ₂ H ₃	I2/m	Adapted from Ni structure from Ref.[4]

Table 4: Co Structures Studied

Compound	Space Group	source
NiH	Fm $\bar{3}$ m	[4]
NiH ₂	Fm $\bar{3}$ m	Adapted from Co structure from Ref.[13]
	I4/mmm	Adapted from Co structure from Ref.[13]
NiH ₃	Pm $\bar{3}$ m	Adapted from Co structure from Ref.[13]
	Pm $\bar{3}$ n	Adapted from Fe structure from Ref.[12]
NiH ₄	Cmmm	Adapted from Fe structure from Ref.[14]
	Immma	Adapted from Fe structure from Ref.[15]
	P21m	Adapted from Fe structure from Ref.[12]
	P213	Adapted from Fe structure from Ref.[15]
NiH₅	I4/mmm	Adapted Fe structure from Ref.[14]
NiH ₆	C2/m	Adapted from Fe structure from Ref.[2]
	Cmmm	Adapted from Fe structure from Ref.[2]
NiH ₇	P63mcm	Adapted from Mn structure from Ref.[1]
	P63mmn	Adapted from Mn structure from Ref.[1]
NiH ₈	P$\bar{1}$	Adapted from Mn structure from Ref.[1]
Ni₃H₅	Pmmm	Adapted from Fe structure from Ref.[2]
Ni ₃ H ₈	Pm $\bar{3}$ m	Adapted from Fe structure from Ref.[2]
Ni₃H₁₃	I4/mmm	Adapted from Fe structure from Ref.[2]
Ni ₂ H ₃	I2/m	[4]

Table 5: Ni Structures Studied

B Code examples

This section contains code examples, relevant for this report, it is not meant to be an exhaustive collection of all the code used. For all code examples as well as the data used in this report, please check Ref. [18].

B.1 VASP

B.1.1 Job Script

Job script for VASP Calculations. This is written to run on the Young computer cluster.

```
#!/bin/bash -l
# Batch script to run an MPI parallel job with the upgraded software
# stack under SGE with Intel MPI.

# 1. Force bash as the executing shell.
#$ -S /bin/bash

# 2. Request ten minutes of wallclock time (format hours:minutes:seconds).
#$ -l h_rt=24:00:00

# Budget setting
```



```

#$ -P Gold
#$ -A UKCP_ED_P

# 3. Request 1 gigabyte of RAM per process.
#$ -l mem=1G

# 5. Set the name of the job.
#$ -N CoH-3m-Wang

# 6. Select the MPI parallel environment and processes.
#$ -pe mpi 80

# 7. Set the working directory to the current directory.
#$ -cwd

# 8. Run our MPI job. GERun is a wrapper that launches MPI jobs on our clusters
# Adjust VASP location to your local setup
VASPBIN=$HOME/vasp_std
oneapi/mkl/latest/lib/intel64:$LD_LIBRARY_PATH

oldpress=0
for press in 0.001 $(seq 50 50 450) $(seq 500 100 3000); do

mkdir -p $press
cd $press

# set up VASP inputs:
sed "/PSTRESS/s/./$press/g" ../INCAR > INCAR
cp ../KPOINTS .
cat ../POTCAR > POTCAR

# set up crystal structure:
if [ -s CONTCAR ]; then
    cp CONTCAR POSCAR
else if [ -s ../$oldpress/CONTCAR ]; then
    cp ../$oldpress/CONTCAR POSCAR
else
    cp ../CoH-Fm-3m-Wang2018-p-1atm.vasp POSCAR
fi
fi

# Run the program

rm out-press-$press
for iter in $(seq 1 5); do

```

```

gerun $VASPBIN >> out-press-$press
# For CP-lab/studentrun, use this command instead:
#mpirun -np 4 $VASPBIN >> out-press-$press

# An option to catch symmetry failures in the VASP run
grep 'VERY BAD' out-press-$press
if [ $? == "0" ]; then

    echo "ISYM = 0" >> INCAR
    echo "NEED TO SET ISYM = 0" >> out-press-$press
    sed -i "/VERY BAD/d" out-press-$press

    gerun $VASPBIN >> out-press-$press
fi

cp CONTCAR CONTCAR-$iter
cp OUTCAR OUTCAR-$iter
cp CONTCAR POSCAR

done
cd ..
oldpress=$press

done

```

B.1.2 INCAR

INCAR code used to perform the constant pressure structure optimization using VASP.

```

# output options
LWAVE = .FALSE. # write or don't write WAVECAR
LCHARG = .FALSE. # write or don't write CHG and CHGCAR
LELF = .FALSE. # write or don't write ELF

# constant pressure geometry optimisation
IBRION = 1      # GO algorithm: 2=conjugate gradient, 1=Newton like
NSW = 100      # number of GO steps
ISIF = 3       # GO settings: 3=relax everything, 2=relax ions only, 4=keep volume
# pressure to optimise towards (in kbar):
PSTRESS = 100

# precision parameters
EDIFF = 1E-6    # SCF energy convergence (eV/cell)
EDIFFG = -1E-3  # Atomic force convergence (eV/Ang)
PREC = high     # Generic precision setting: low, med, high, accurate

```

```

# plane wave cutoff energy
ENCUT = 800

# electronic relaxation
ISMEAR = 0      # Smearing algorithm: -5 = Tetrahedron, 0 = Gaussian,
                # 1..N = Methfessel
SIGMA = 0.1     # Smearing width in eV

# parallelisation setting
# Young cluster:
NCORE = 10
# CP-Lab/studentrun:
#NCORE = 4

```

B.1.3 KPOINTS

K-point grid for VASP calculations.

```

Auto
0
Auto
40

```

B.2 Quantum Espresso

B.2.1 SCF Calculation

Example code for the SCF calculation done in quantum espresso.

```

&control
  calculation='scf'
  restart_mode='from_scratch',
  prefix='FeH',
  pseudo_dir = './',
  outdir='FeH-bcs/',
/
&system
! Enter crystal structure information below
 ibrav= 1
  !space_group = 225
  cellldm(1) = 3.4419202805
  ntyp= 2
  nat=8
! Edit plane wave cutoff below if necessary
  ecutwfc = 90.0,
  occupations = 'smearing',
  smearing = 'methfessel-paxton',

```

```

        degauss=0.02,
        la2F = .true.
/
&electrons
    conv_thr = 1.0d-6,
    mixing_beta = 0.7
/
ATOMIC_SPECIES
Fe 55.845 Fe.pbe-spn-rrkjus_psl.1.0.0.UPF
H  1.008 H.pbe-rrkjus_psl.1.0.0.UPF

ATOMIC_POSITIONS {crystal}

Fe 0.0000000000      0.0000000000      0.0000000000
Fe 0.0000000000      0.5000000000      0.5000000000
Fe 0.5000000000      0.0000000000      0.5000000000
Fe 0.5000000000      0.5000000000      0.0000000000
H  0.5000000000      0.5000000000      0.5000000000
H  0.5000000000      0.0000000000      0.0000000000
H  0.0000000000      0.5000000000      0.0000000000
H  0.0000000000      0.0000000000      0.5000000000

K_POINTS {automatic} ! Edit k-grid size below
8 8 8 0 0 0

```

B.2.2 Phonon Calculation

```

&inputph
    tr2_ph=1.0d-6,
! Some directory and file name definitions:
    prefix='FeH',
    fildvscf='FeH_dv',
    outdir='FeH-bcs/',
    fildyn='FeH.dyn',
    alpha_mix(1)=0.1,

! recover = .true.,
! Atomic masses of atoms
! WARNING: the order of these needs to
! be consistent with the SCF input files

amass(1)=55.845,
amass(2)=1.008,

! Electron-phonon coefficients

```

```

    electron_phonon='interpolated',
    trans=.true.,
    ldisp=.true.

! q-point grid on which to perform DFPT
    nq1=8, nq2=8, nq3=8
/

```

B.2.3 Post Processing Calculations

q2r input file :

```

&input
    zasr='simple',
! File name conventions
! Need to be consistent with
! FeH.elph.in!
    fildyn='FeH.dyn',
    flfrc='FeH.fc',
    la2F=.true.
/

    matdyn input file

&input
    asr='simple',

! Atomic masses of atoms
! WARNING: the order of these needs to
! be consistent with the SCF input files
    amass(1)=55.845,
    amass(2)=1.008,

! File name conventions
! Must be consistent with
! h3s.q2r.in
    flfrc='FeH.fc',
    flfrq='FeH.freq',
    la2F=.true.,
    dos=.true.
    fldos='FeH.dos',
    q_in_band_form = .true.,

! q-grid for phonon evaluation
    nk1=10, nk2=10, nk3=10,
    ndos=50
/

```

C Densities of States

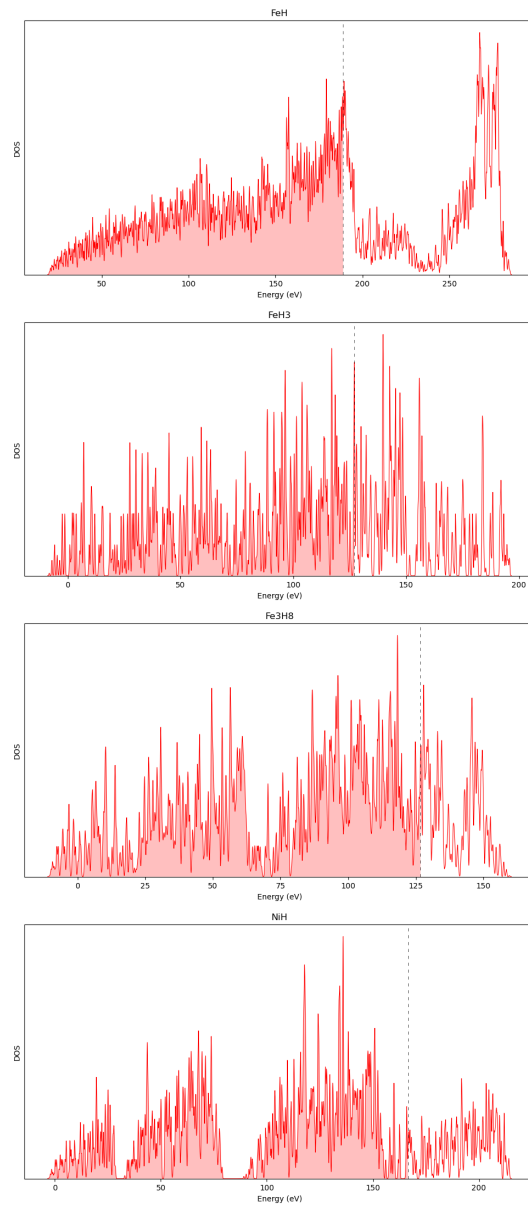


Figure 7: Densities of States Plots